Reaction mechanisms of the $^{18}O + ^{63}Cu$ system at near-barrier energies

E. Crema,[1,*] V. A. B. Zagatto,[2] J. M. B. Shorto,[3] B. Paes,[2] J. Lubian,[2] R. F. Simões,[1] D. S. Monteiro,[4,5] J. F. P. Huiza,[6] N. Added,[1] M. C. Morais,[7] and P. R. S. Gomes[2,†]

[1]*Instituto de Física, Universidade de São Paulo, 05315-970 São Paulo, Brazil*
[2]*Instituto de Física, Universidade Federal Fluminense, 24210-340, Niterói, Rio de Janeiro, Brazil*
[3]*Instituto de Pesquisas Energéticas e Nucleares, IPEN/CNEN, 05508-000, São Paulo, SP, Brazil*
[4]*ILACVN, Universidade Federal da Integração Latino Americana, 85866-000, Foz do Igaçu, PR, Brazil*
[5]*Department of Physics, University of Notre Dame, 46556, South Bend, Indiana, USA*
[6]*Universidade Estatual do Sudoeste da Bahia, Bahia, Brazil*
[7]*INFES, Universidade Federal Fluminense, Santo Antônio de Pádua, Rio de Janeiro 28470-000, Brazil*

(Received 6 June 2018; revised manuscript received 27 August 2018; published 17 October 2018)

A precise quasielastic excitation function for the $^{18}O + ^{63}Cu$ system has been measured at energies around the Coulomb barrier at $\theta_{LAB} = 161^{\circ}$. The corresponding quasielastic barrier distribution has been derived. Two-neutron-, one-proton-, and α-transfer-excitation functions have also been measured at the same energies and angle. Coupled reaction channels calculations were performed to describe the experimental data. Large-scale shell-model calculations were performed to derive most of the spectroscopic amplitudes. No surface imaginary potential was necessary for the interaction potential because almost all relevant reaction channels were explicitly included in the calculation. The theoretical results were compared to the experimental quasielastic barrier distribution and a very good agreement was achieved. The comparison of the coupled reaction channel calculations and data has put in evidence several important details of the reaction mechanism of the $^{18}O + ^{63}Cu$ system. The collectivity of the ^{63}Cu nucleus has important contribution to the reaction mechanism of this system, mainly due to its first $5/2^+$ and $7/2^+$ states. It was also observed a striking influence on the reaction dynamics of the $^{18}O(2^+)$ state, the two-neutron transfer and the reorientation of the target ground-state spin. The best agreement to data was achieved when the nuclear matter diffuseness for the ^{18}O was assumed equal to 0.60 fm, value that we have derived in a previous paper and that is 10% greater than the ^{16}O diffuseness. Another significant result was that the two-neutron transfer process is much more relevant than the one-neutron-transfer process, which suggests that the pairing correlation could play an important role in the transfer process of this system.

DOI: 10.1103/PhysRevC.98.044614

I. INTRODUCTION

Quasielastic barrier distribution measured at backward angles is a tool that has been successfully employed to study both nuclear structure and nuclear reaction mechanism [1–11]. At low energies, when tightly bound nuclei are involved, quasielastic scattering is defined as the sum of elastic scattering, inelastic scattering, and all direct transfer reactions. Very precise quasielastic data are required to deduce a quasielastic barrier distribution (QEBD) because a derivative of data is involved. The QEBD is obtained by $-d(\sigma_{qel}/\sigma_{Ruth})/dE$, where $d\sigma_{qel}$ is the quasielastic differential cross section and σ_{Ruth} is the Rutherford cross section [3]. When these data are taken at backward angles, the quasielastic events detected are populated mainly by the lowest partial waves that deeply interact with the target. Consequently, barrier distributions are very sensitive to the interaction potential details, and they are very useful to disentangle the relative importance of the different reaction channels in the distribution of the reaction flux [12]. Besides, fusion barrier distribution and QEBD for tightly medium-mass nuclei are similar at energies around the Coulomb barrier, since quasielastic and fusion are complementary processes, fed by the same partial waves and carry almost the same information [4–6]. However, as pointed out by Timmers *et al.* [4], at energies well above the average barrier energy, the QEBD for some systems tends to lose sensitivity due to the domination of the reaction channels at these energies. In addition, the derivative of the excitation function can put in evidence details of processes that are not easily observed in the original excitation function. In this paper, we take advantage of these properties of the QEBD to investigate the reaction mechanism of the $^{18}O + ^{63}Cu$ system, in which we are particularly interested in the neutron-transfer process.

In recent years, there has been a renewed interest in the study of few- and multinucleon transfer processes to better understand the transition between deep inelastic scattering and the quasielastic collisions [13–15]. Besides, as more detailed and fundamental calculations are available, several papers have been also dedicated to investigating the role of

*crema@if.usp.br
†Deceased.

the pairing interaction during transfer processes [16–21]. We have shown that the pairing correlation plays an important role in the reaction mechanism of the ^{48}Ca + ^{120}Sn system [11]. The projectile ^{18}O has been frequently chosen in this kind of research because its neutron pair outside the ^{16}O core is relatively easy to be transferred to another nucleus even in collisions at energies near the Coulomb barrier. In addition, as the ^{16}O core is very stable, it does not participate actively in the reaction mechanism at low bombarding energies. In this paper, the ^{63}Cu target was chosen because its outer $1f_{5/2}$ neutron sublevel is occupied by only two neutrons, and there is room in this sublevel to accept the two neutrons from the projectile. In the next step of this systematic study, we will use the nucleus ^{65}Cu as a target to investigate the role of the $1f_{5/2}$ sublevel occupancy on the reaction mechanism.

In theoretical calculations of reactions that involve heavy nuclei, one should be very careful in the choice of the model. For instance, as it is well known, the distorted-wave Born approximation (DWBA) is only an appropriate choice when the elastic scattering is the dominant reaction channel, which could not be the case at energies well above the Coulomb barrier. In the present paper, large-scale coupled reaction channel (CRC) calculations were performed to analyze the experimental transfer excitation functions, and to put in evidence the most relevant channels in the reaction mechanism of the ^{18}O + ^{63}Cu system.

On the other hand, in a previous paper [10], we have derived the nuclear matter diffuseness of the nucleus ^{18}O, and the result was, approximately, 10% larger than the ^{16}O one. With the present paper, we can confirm that result. This diffuseness value is very important for our calculations because the choice of the real interaction potential is a crucial point of our method, described elsewhere [7–11]. No imaginary potential at the interaction surface is employed, and the real interaction is a double-folding potential calculated with a two-parameter Fermi shape for the matter and charge densities, the so-called São Paulo potential (SPP) [22]. As the radius and diffuseness parameters of the SPP have been calculated averaging hundreds of experimental and theoretical values, our real potential is parameter free in this sense. To account for the fusion process, an inner (to the nominal Coulomb barrier) imaginary Woods-Saxon potential was used, in such a way that variation of its parameters does not affect the results. So, as we were not fitting data, our theoretical results are to be compared to data.

This paper is organized as follows. In Sec. II, the details of the experimental facility at the São Paulo University are given. The details and discussion of our theoretical results are given in Sec. III. Finally, the main conclusions of our work are presented in Sec. IV. Details about the shell-model calculations may be seen in the Appendix.

II. EXPERIMENT

Measurements were made at the Pelletron Laboratory of the University of São Paulo. The beams of ^{18}O were accelerated by its 8 UD electrostatic accelerator in the energy range of $E_{\rm lab} = 30.0$–48.0 MeV, in steps of 1 MeV, with intensities from 10–100 pnA. The beams were deflected by a 90° analyzing magnet and their energies were defined with an uncertainty of the order of 40 keV. The self-supporting target of 80 μg/cm^2 of ^{63}Cu isotope was enriched to 99.9%. The reaction products were detected and identified by a conventional E-ΔE proportional counter placed at $\theta_{\rm LAB} = 161°$, where the ΔE signal was provided by the gas mixture P-10 at a pressure of 15 torr. The residual energies of the reaction products were measured by a silicon surface barrier detector placed behind the gas detector. The projectilelike fragments detected by the proportional counter were normalized to Rutherford scattering events detected by three surface barrier detectors placed at forward angles (±30° and 45°). These three normalization processes gave very similar cross sections for each measured reaction channel. As usual in experiments to measure barrier distributions, before starting data acquisition, the magnet was properly recycled. The statistical uncertainties for the quasielastic excitation function were below 1% for most energies, and, for the highest energies, around 3%. A typical E-ΔE spectrum, taken at $E_{\rm lab} = 40.0$ MeV, is shown in Fig. 1, where the different projectilelike fragments are separated according to their charge.

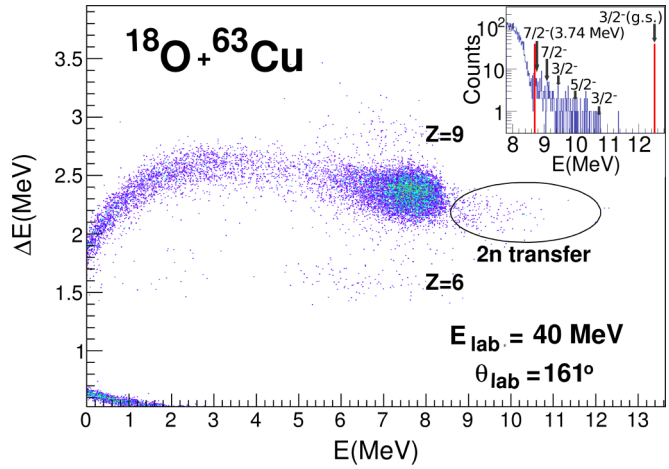

FIG. 1. Typical E-ΔE spectrum of the ^{18}O + ^{63}Cu system taken at $E_{\rm lab} = 40$ MeV and at $\theta_{\rm lab} = 161°$.

As indicated in Fig. 1, the fragments with $Z = 6$ and 9, which correspond to transfer processes, were well identified and their excitation functions could also be measured. The group of events indicated as $Z = 8$ in the figure contains the elastic, the inelastic and the one- and two-neutron transfer processes. The events with energies higher than the elastic events are produced by the two-neutron stripping process, which has Q value between ground states $Q_{gg} = 5.64$ MeV, and its excitation function could also be also measured. However, only the two-neutron transfer events between states with excitation energies lower than approximately 3.8 MeV are distinguished from the elastic events. In the past, we measured the system ^{16}O + ^{63}Cu [8] and these two-neutron transfer events, and $Z = 9$ events as well, are completely absent. On the other hand, in the present experiment, as the one-neutron stripping process has $Q_{gg} = -0.13$ MeV, its events cannot be separated from the elastic ones. As the main focus of this study was to measure the quasielastic barrier distribution,

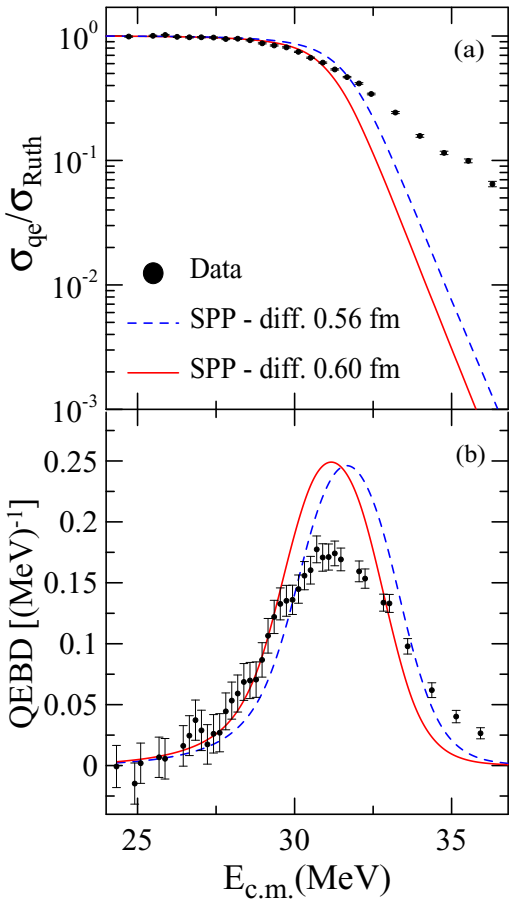

FIG. 2. Calculations comparing the effect of different nuclear ^{18}O mass diffuseness on (a) quasielastic excitation function of the $^{18}O + ^{63}Cu$ system, and (b) its corresponding quasielastic barrier distribution (see text for details).

a high-precision excitation function measured at backward angles was required. For this purpose, the angular acceptance of the E-ΔE detector was intentionally increased to improve the statistics. As a consequence, the energy resolution was not good enough to separate the elastic events from the inelastic ones. This was not a limitation of the experiment because we were interested in the inclusive quasielastic events and the energy cutoff used in our analysis guarantee that all inelastic events with excitation energies up to 7 MeV were taken into account. Finally, the measured quasielastic excitation function and its corresponding QEBD are shown in Fig. 2.

III. THEORETICAL CALCULATIONS

Theoretical calculations have been performed for the $^{18}O + ^{63}Cu$ system to study the effect engendered by each reaction channel on the quasielastic excitation function (EF) and its corresponding QEBD. The inelastic channels have been described in the view of the coupled channels (CC) formalism, while the effects of the transfer channels have been studied using the coupled reaction channels (CRC) method. Both kinds of calculations were performed using code FRESCO [23]. A key ingredient for properly describing the transfer partitions is the spectroscopic amplitudes (SAs) of projectile and target overlaps. Usually, for determining such transition amplitudes, one measures the experimental cross sections and adjusts the SA in calculations to describe the angular distribution of a specific final channel, using the DWBA. This procedure has been a useful tool through the years. However, it may hide deeper effects, such as sequential transfers or effects of collective excitations of the interacting nuclei, not allowing us to distinguish among different reaction mechanisms. To avoid this, the SAs of the present paper have been determined theoretically by shell-model calculations with the code NUSHELLX [24], whenever it was possible.

In all the following calculations, the real nuclear potential on the entrance partition ($^{18}O + ^{63}Cu$) will be given by the double-folding São Paulo potential (SPP) [22]. A characteristic of this nuclear potential is its low dependence with the bombarding energy, and it is possible to consider it as energy independent in the energy range investigated in this paper. To simulate the fusion process, an inner (to the Coulomb barrier) imaginary Woods-Saxon (WS) potential has been adopted. The WS parameters adopted were $V_i = 80$ MeV, $r_i = 0.8$ fm, and $a_i = 0.6$ fm, as proposed in Ref. [8]. One may notice that there are no imaginary superficial potentials in the calculations, meaning that superficial processes, such as transfer and inelastic excitations, are not taken into account via any optical potential. In the final partitions of all CRC calculations performed in this paper, the São Paulo potential was used for both, real and imaginary part of the optical potential, with normalizations of 1.0 and 0.78, respectively. This is in accordance with the São Paulo systematics proposed in Refs. [25,26], which has already been proven to be appropriate to describe the elastic scattering of several systems in a wide energy range. This prescription is valid if no explicit couplings were included in the final partitions. A real Woods-Saxon potential with $r_o = 1.2$ fm and diffuseness $a = 0.75$ fm was used to bind the valence particle to its respective core. The depth of the Woods-Saxon potential was varied to reproduce the experimental binding energies. A spin-orbit interaction has also been considered in the cases where the valence particle had nonzero spin. Prior representation of the effective potential was used in our finite-range CRC calculations considering complex remnant.

There are important structural differences among the stable oxygen isotopes that must be incorporated into calculations. Such differences may be taken into account through the nuclear potential. Particularly, the SPP uses a systematic constant value ($a = 0.56$ fm) for calculating the nuclear mass diffuseness. Previous papers [10,27] have demonstrated that the ^{18}O presents an enhanced diffuseness ($a = 0.6$ fm) compared to its most abundant isotope, ^{16}O, because of the addition of the two neutrons in the valence subshell. That larger diffuseness strongly affects the EF and the QEBD, as may be seen in Fig. 2, where it is shown that this static effect produces a decrease of the nominal fusion barrier by about 1 MeV. The value $a = 0.60$ fm for the diffuseness of the matter distribution of the ^{18}O nucleus will be adopted from now on. In the next sections, the dynamic effects that emerge from the coupling of channels on the quasielastic excitation function and the derived QEBD will be presented.

TABLE I. Reduced transition probabilities (in W.u.) for the transition between the initial and final states of spins and parity I_i and I_f of ^{63}Cu, respectively. The energies of initial and final states are also shown.

I_i	E_{Initial} (MeV)	I_f	E_{Final} (MeV)	$B(E2)$ (W.u.)
$3/2^-$	0	$1/2^-$	0.699	15.2
$3/2^-$	0	$5/2^-$	0.962	15.7
$3/2^-$	0	$7/2^-$	1.326	12.7
$3/2^-$	0	$5/2^-$	1.412	1.0
$1/2^-$	0.699	$5/2^-$	1.412	6.0
$3/2^-$	0	$3/2^-$	1.547	3.7
$3/2^-$	0	$7/2^-$	1.86	1.4
$3/2^-$	0	$7/2^-$	2.092	0.3
$3/2^-$	0	$7/2^-$	2.404	0.2

First, the inelastic channels will be considered, then CRC calculations will be employed to describe the experimental two-neutron-, proton-, and α-transfer excitation functions that we have measured in this work. Finally, the effect of the one-neutron-transfer process on the EF and QEBD will be theoretically investigated.

A. Inelastic couplings

Several inelastic channels have been included in the coupling scheme of the CC calculations. As the quasielastic experimental peak presented a width of 2 MeV, the main states of projectile and target within this energy range have been included in the coupling scheme. The states of the target that have been considered are listed in Table I. The experimental reduced transition probabilities [$B(E2)\uparrow$] were obtained from Ref. [28]. The coupling potentials are taken as the first derivative of the Coulomb and nuclear real potentials. The adopted transitions and respective $B(E2)\uparrow$ used in calculations are presented in Table I.

These experimental reduced transition probabilities have been used to calculate the nuclear and Coulomb coupling matrix elements. The reorientation effect of the ground state (g.s.) of the ^{63}Cu was also considered, and the experimental value of the electric quadrupole moment for the nucleus ^{63}Cu ($Q = 22.0$ fm) was obtained in Ref. [29]. The projectile first excited state, ^{18}O(2^+) at 1.982 MeV, has also been included in the coupling scheme with $B(E2)\uparrow = 16.1$ W.u. that was reported in Ref. [30].

An analysis of the importance of each inelastic channel and how it affects the QEBD and the EF has been performed. The results are shown in Fig. 3, where only the channels that significantly affect the calculations are presented. One must notice that the individual effect of each channel is not shown in these figures. What is shown is the cumulative effect of new higher excited states of the target, and then of the first excited state of the projectile. The reorientation effect of the g.s. of the target was the last one to be considered. The QEBD and EF are mostly affected by the coupling of the three first inelastic states of target:$1/2^-$ ($E = 0.669$ MeV), $5/2^-$ ($E = 0.962$ MeV), and $7/2^-$ ($E = 1.326$ MeV), which are represented in the figure by the green, blue, and magenta

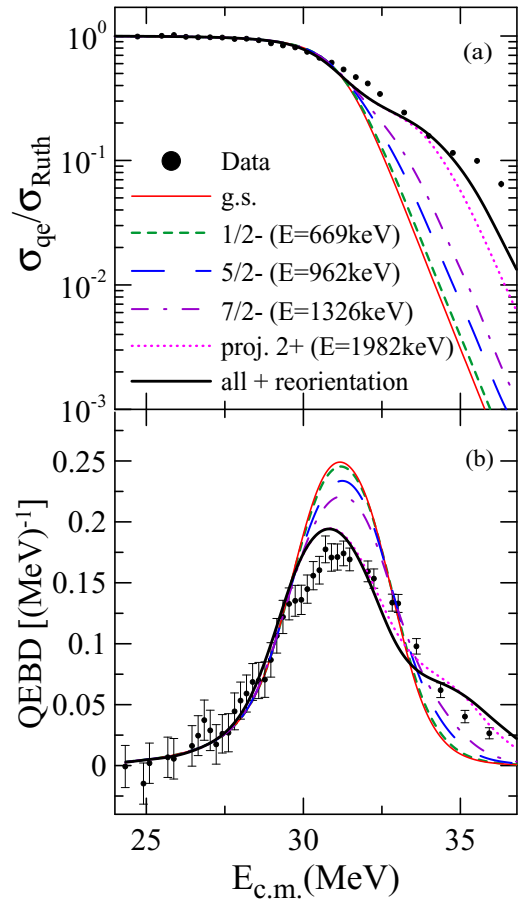

FIG. 3. Results of the coupled channel calculations comparing the effect generated by the coupling of the most relevant inelastic channels on (a) quasielastic excitation function of the ^{18}O + ^{63}Cu system, and (b) its corresponding quasielastic barrier distribution (see the text for details).

dashed lines, respectively. Besides them, the pink dotted line shows that the excitation of the projectile (2^+ at 1.982 MeV) strongly affects the QEBD at energies around the barrier, and the EF at energies above the barrier. Finally, as shown by the black solid line, the reorientation of the g.s. of the target also has a significant effect on EF, especially at energies above the Coulomb barrier. However, the reorientation has a negligible influence on QEBD at the barrier energy region.

B. Two-neutron transfer

The two-neutron stripping process may be clearly identified in the spectra of Fig. 1 since their events are located to the right of the elastic peak. This is consistent with the positive Q value of this channel of +5.6 MeV. With the Q-optimum value obtained by the Brink's rule [31], the expected excitation energy of the ^{65}Cu is up to 5 MeV. This high excitation energy of the ^{65}Cu generates several problems when one tries to describe the nuclear structure of this nucleus by microscopic calculations. The first problem is the necessity to employ an extremely large model space, which allows describing the low-lying and high excited states of a given

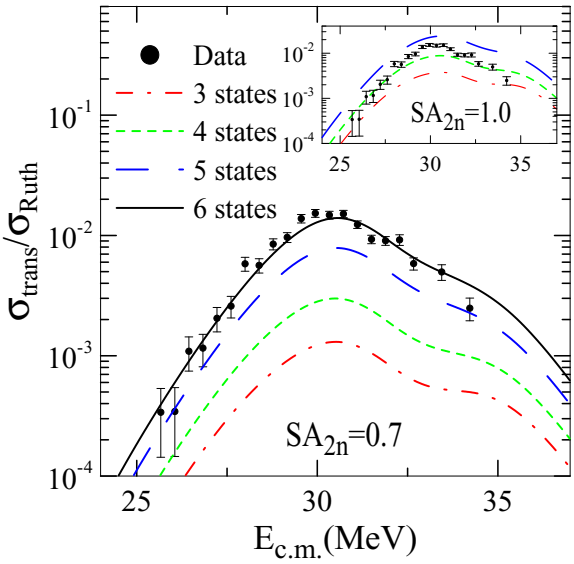

FIG. 4. Two-neutron-transfer data. The different lines represent the sums of the given number of states of the ^{65}Cu nucleus. The CRC calculations were performed using the overall spectroscopic amplitudes of the two-neutron transfer process set to 0.7. The inset shows the same calculations when the spectroscopic amplitudes are set to 1.0.

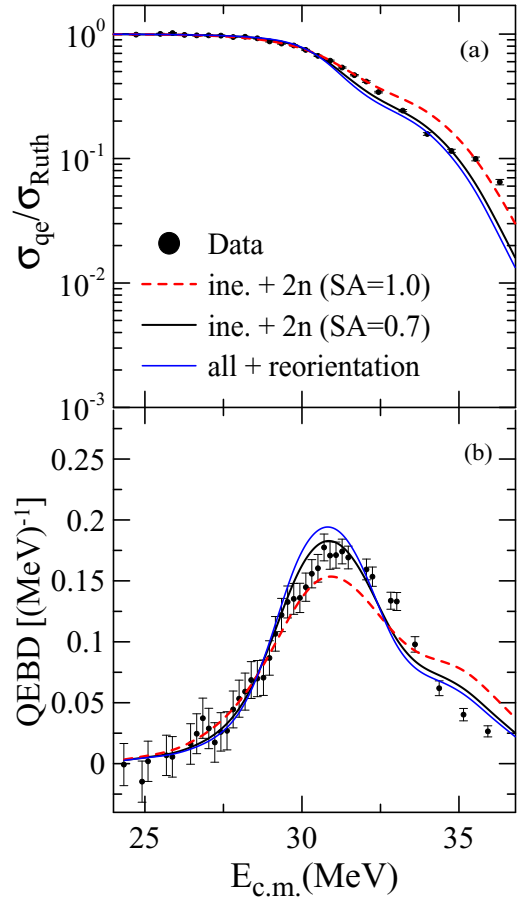

FIG. 5. CCC and CRC calculation for the $^{18}O + ^{63}Cu$ system including inelastic excitations and two-neutron-transfer processes. The reaction effects of the inclusion of these channels are shown in (a) quasielastic excitation function, and (b) quasielastic barrier distribution (see the text for details).

nucleus simultaneously. There is also a problem because of the high density of states in such energy range for the ^{65}Cu nucleus. Many of these states do not have their spin-parity values well determined experimentally. These difficulties turn very hard, or even not possible, to perform shell-model calculations to determine the spectroscopic amplitudes for this large amount of states. The solution adopted in this reaction is to perform CRC extreme-cluster calculations, considering the two neutrons as a single particle (dineutron) bound to the ^{16}O core. In such an approximation, the two neutrons are paired antiparallel, and the internal structure of the associated particle is neglected. In this way, the spin assigned to the transferred dineutron is 0. Although it is an approximation, this cluster model still provides valuable information about pairing effects or structural information of the involved nuclei.

The calculations have been guided by the experimental information present in the $2n$-transfer spectrum because of the large number of states in this high energy range of the ^{65}Cu excitation spectrum. The panel inserted in Fig. 1 shows a spectrum of the $Z = 8$ events in the energy region that corresponds to the two-neutron-transfer processes, where its integration limits are signed by the red lines, which account for the events produced when the ^{65}Cu is left with excitation energies up to 3.8 MeV. As shown in Fig. 4, the experimental two-neutron-transfer excitation function has been measured, and it will be very helpful in the following theoretical analysis. From the calibration of the detector, it was possible to estimate the approximate energy of the most intense peaks related to this transfer. An analysis of the known spectrum of the ^{65}Cu, and its experimentally well determined levels (at this same energy region) have leaded to the inclusion of six states of the ^{65}Cu on the coupling scheme: 3/2- (g.s.), 3/2- ($E =$ 1.725 MeV), 5/2- ($E = 2.593$ MeV), 3/2- ($E = 3.079$ MeV), 7/2- ($E = 3.427$ MeV), and 7/2- ($E = 3.740$ MeV), which are indicated by the arrows in the inset in Fig. 1.

The first attempt in the extreme cluster model consisted for using SA set equal to 1.0 for all the transitions. The panel inserted in Fig. 4 shows the results of these CRC calculations that include progressively five of the six states of the ^{65}Cu mentioned before. As one can see by the blue long-dashed line in the inset of the figure, the CRC calculations using spectroscopic amplitudes equal to 1.0, and coupling the five states (up to 3.74 MeV), has overestimated the experimental data in the whole energy range. However, the shape of the energy dependence of the two-neutron-transfer process is well reproduced by these calculations, which indicates that the assumed values for the SA should be too large. These theoretical results can also be observed in the EF and QEBD shown in Fig. 5, where the red dashed line is the CRC calculation with the overall SA equal to 1.0, and the blue solid line represents the calculation that couples only the inelastic channels. One can see in this figure that the theoretical barrier distribution does not agree with the data.

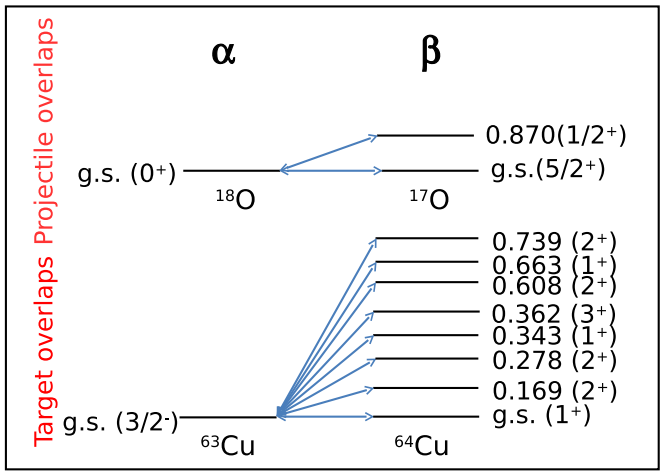

FIG. 6. Coupling scheme adopted in CRC calculations for the ^{18}O (^{63}Cu, ^{64}Cu) ^{17}O reaction.

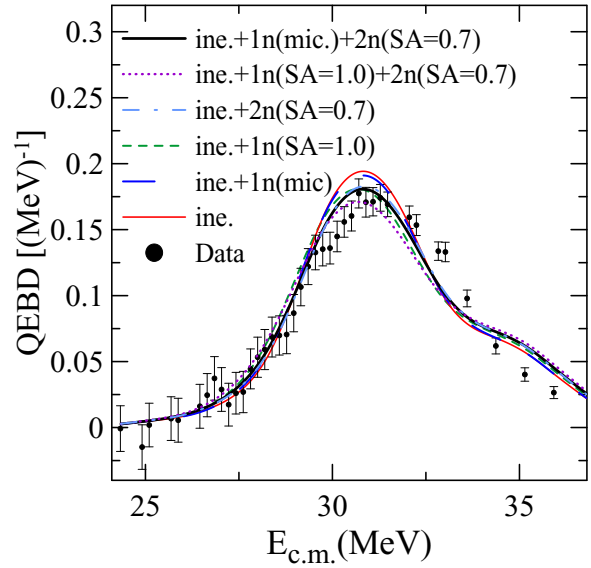

FIG. 7. CCC and CRC calculation for the $^{18}\mathrm{O} + {}^{63}\mathrm{Cu}$ system including inelastic excitations, one- and two-neutron-transfer processes. The reaction effects of the inclusion of these channels are shown in the quasielastic barrier distribution (see the text for details).

In Ref. [19], the two-neutron stripping transfer from the ^{18}O projectile to the ^{62}Ni target was studied. It was shown that the calculations with the extreme-cluster model (with SA = 1.0) overestimate the experimental data for the transitions to the ground state, and the first excited state of the ^{64}Ni. As the copper and nickel isotopes are close to each other, this may indicate the necessity to decrease the SAs for the ^{63}Cu case as well. After some tests, the value SA = 0.7 has been adopted for all overlaps of the present reaction. As can be seen by the black solid line in Figs. 4 and 5, the experimental excitation function is very well adjusted by this approach. So, from now on, we will assume SA = 0.7 for all transitions of the two-neutron-transfer calculations.

C. One-neutron transfer

Differently from the two-neutron-transfer channel, the one-neutron-transfer events are not isolated in the spectrum shown on Fig. 1 because their low Q values ($Q_{gg} = -0.129$ MeV) do not allow us to kinematically separate them from the elastic events. So, without transfer data to guide the analysis of the CRC calculations for the one-neutron transfer, we will use the sensitivity of the QEBD to investigate the effect of this channel on the reaction mechanism. The one-neutron transfer has also been included in calculations through CRC theoretical formalism. The projectile/ejectile coupling scheme considered the overlaps of the g.s. of the of projectile ^{18}O with the g.s. and the first excited state ($1/2^+$ with $E = 0.870$ MeV) of the ^{17}O. Calculations revealed that the effect on QBED and EF coming from the ejectile left in its first excited state is negligible because the cross section is about two orders of magnitude lower than the one that emerges from the situation where the ejectile remains in its ground state. All the states of the residual nucleus ^{64}Cu with excitation energy up to 2 MeV, and for which there are experimentally well-determined spin, parity, and reduced transition probability have been included in the calculations. Seven excited states of the ^{64}Cu have been included in the coupling scheme, which is depicted in Fig. 6.

One should keep in mind that the good agreement of data with the previous calculations of two-neutron-transfer reaction indicates that the effect of including the one-neutron stripping in the coupling scheme must be small. This conclusion was indirectly validated by the experimental data of two-neutron transfer. As we do not have experimental data from one-neutron-transfer process to confirm that conclusion, only a theoretical analysis can be done. So, two different sets of spectroscopic amplitudes have been used in the calculations. First, all of them were set SA = 1.0. This was done to check the maximum effect that the one-neutron stripping process could have on the EF and the QEBD. The EF was not sensitive to all calculations discussed in this section, and it will not be shown in the figures. However, owing to the sensitivity of barrier distributions, one could investigate the effects of these different calculations on the reaction mechanism. For instance, the green dashed line in Fig. 7 shows that there is an important effect of the inclusion of the one-neutron transfer in the CRC calculation assuming all of its SA = 1.0. This calculation produces a QEBD like that obtained with two-neutron transfer with SA = 0.7 shown in Fig. 5. However, when these one- and two- neutron transfers are included together in the CRC calculation, the agreement of the theoretical cross section with data became worse, as shown by the magenta dotted line in the Fig. 7, which indicates that the attempt SA = 1.0 was an overestimation of the spectroscopic amplitudes for the one-neutron-transfer process, because the values SA = 0.7 for the two-neutron transfer has already been confirmed by experimental data, as was shown in Fig. 4. The next and natural step of our analysis was to include in the CRC calculation, besides the inelastic excitations, both the two-neutron transfer (with SA = 0.7) and the one-neutron transfer with the calculated microscopic spectroscopic factors. Shell-model calculations have been performed with NUSHELLX

TABLE II. Spectroscopic amplitudes used in the CRC calculations for $^{17}O + ^{64}Cu$ partition. nn, l, and j are the quantum numbers of the neutron orbitals for the one-neutron-transfer reaction.

Intial	Final	*nn*	*I*	*j*	A_{isJ}
^{18}O-0^+	^{17}O-$5/2^+$	1	2	2.5	1.272
^{18}O-0^+	^{17}O-$1/2^+$	2	0	0.5	0.445
^{63}Cu-$3/2^-$	^{64}Cu-1^+	2	1	0.5	−0.075
		2	1	1.5	0.1266
		1	3	2.5	−0.581
^{63}Cu-$3/2^-$	^{64}Cu-2^+	2	1	0.5	0.0034
		2	1	1.5	−0.237
		1	3	2.5	0.6555
^{63}Cu-$3/2^-$	^{64}Cu-$2(2)^+$	2	1	0.5	−0.043
		2	1	1.5	−0.267
		1	3	2.5	−0.373
^{63}Cu-$3/2^-$	^{64}Cu-$1(2)^+$	2	1	0.5	−0.137
		2	1	1.5	0.1329
		1	3	2.5	−0.045
^{63}Cu-$3/2^-$	^{64}Cu-3^+	2	1	1.5	−0.07
		1	3	2.5	−0.853
^{63}Cu-$3/2^-$	^{64}Cu-$2(3)^+$	2	1	0.5	0.2728
		2	1	1.5	−0.168
		1	3	2.5	−0.128
^{63}Cu-$3/2^-$	^{64}Cu-$1(3)^+$	2	1	0.5	−0.729
		2	1	1.5	−0.18
		1	3	2.5	0.1744
^{63}Cu-$3/2^-$	^{64}Cu-$2(4)^+$	2	1	0.5	0.6014
		2	1	1.5	−0.152
		1	3	2.5	−0.073

code to calculate these microscopic SAs. These calculations will be discussed in the Appendix. To our knowledge, there are no papers in the literature that report the SAs of the $^{63,64}Cu$ nuclei. The black solid line in Fig. 7 shows that a very good agreement is attained between the results of this CRC calculation and the experimental QEBD. A comparison of this calculation with the other that uses SA = 1.0 reveals an improvement of the reduced chi-square (χ^2_{red}) value. When the SA = 1.0 is employed, we obtained $\chi^2_{red} = 3.4$, while for the calculations using microscopic SAs for the one-neutron transfer the $\chi^2_{red} = 2.6$, which shows an improvement.

The results of CRC calculations that consider both projectile and target SAs are shown in Fig. 7. The blue dashed line in this figure reveals that, in fact, the use of microscopic SA causes a significant reduction in the coupling effect of the one-neutron-transfer channel on the QEBD. From nuclear structure calculation, it was obtained that there is an enhancement of the calculated amplitude for the g.s. to g.s. overlap of the projectile (first line of Table II in the Appendix) compared to the SA = 1.0 value used before. From these two facts, it is possible to infer that this reduction of the coupling effect of the one-neutron transfer is correlated mainly to the decreasing of the amplitudes in target/recoil overlaps, which shows the sensitivity of one-neutron stripping effects to the amplitudes of these overlaps.

The previous calculations reveal that the two-neutron transfer is the transfer that most affects the shape of the QEBD.

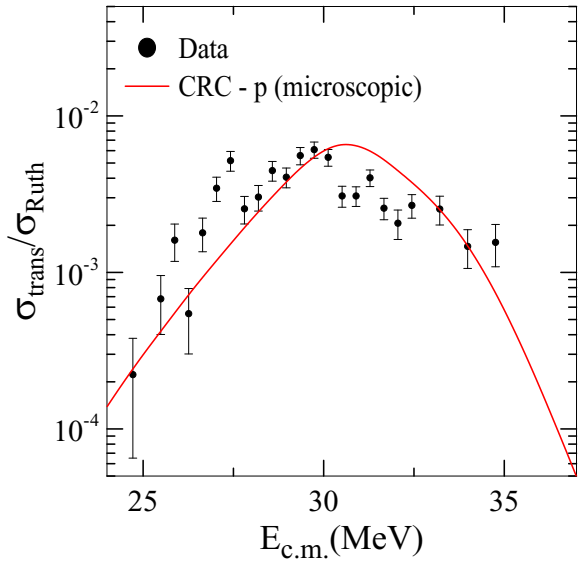

FIG. 8. Proton transfer data. The red line represents the CRC calculation with the sums of the first four states of the ^{62}Ni nucleus.

The effect of one-neutron transfer on the QEBD is strongly reduced when microscopical SA are used. In this case, if one calculates the two-neutron transfer using the sequential CRC method, its effect would be attenuated because of the limitation imposed by the one-neutron process. This last result indicates the absence of competition between short- and long-range correlations. As the direct two-neutron transfer is more intense than the one-neutron process, this may be an indication of the existence of pairing forces between the two transferred neutrons.

D. One-proton transfer

The experimental spectrum of $^{18}O + ^{63}Cu$ shown in Fig. 1 also reveals the presence of events with $Z = 9$ particles, which are related to the production of fluorine isotopes during the interaction process. This kind of reaction is a pick-up process where particles from the target are captured by the projectile. The detectors employed in the data acquisition do not allow us to separate particles in mass, so, it is not possible to determine if such particles have been generated from a proton or a deuteron capture. However, as the Q value for the first process is 1.871 MeV, and it is −2.123 MeV for the later, it is possible to energetically distinguish them in a calibrated spectrum. In our spectra, most of $Z = 9$ events come from the proton pick-up process. The experimental excitation function of this process is shown in Fig. 8.

In the CRC calculations, only the overlap between ground states was adopted for the projectile/ejectile. The first four states of ^{62}Ni have been coupled in the calculations, always considering their overlap with the g.s. of ^{63}Cu. The oxygen and nickel states coupled in the calculations, and their respective SA, are shown in Table III of the Appendix. Our microscopic SAs are compatible with those determined experimentally for the projectile and target overlaps in Refs. [32,33], respectively. The comparison of transfer data with the calcula-

TABLE III. Spectroscopic amplitudes used in the CRC calculations for ^{63}Cu (^{18}O, ^{19}F) ^{62}Ni reaction. nn, l, and j are the quantum numbers of the proton orbitals for the one-proton-transfer reaction. The energies of the final states are also shown in the table.

Intial	Final	E_{Final} (MeV)	nn	I	j	Present A_{isJ}	Literature A_{isJ}
^{18}O-0$^+$	^{19}F-1/2$^+$	0	2	0	0.5	0.5878	0.6(1)
^{63}Cu-3/2$^-$	^{62}Ni-0$^+$	0	2	1	1.5	−0.837	0.7(1)
^{63}Cu-3/2$^-$	^{62}Ni-2$^+$	1.173	2	1	0.5	0.2621	0.55(10)
			2	1	1.5	−0.418	
			1	3	2.5	0.1124	
^{63}Cu-3/2$^-$	^{62}Ni-0$^+$	2.049	2	1	1.5	0.0103	–
^{63}Cu-3/2$^-$	^{62}Ni-2$^+$	2.301	2	1	0.5	0.0557	–
			2	1	1.5	0.0341	
			1	3	2.5	−0.013	

tions may be visualized in Fig. 8, where the red line represents the sum of all four states included in the coupling scheme. One can see that the experimental data are well described by the theoretical predictions (we did not fit any parameters in this case). The main contribution comes from the g.s to g.s transition, which represents more than 90% of the transfer cross section. The first excited state contributes with almost all the rest of the cross section, while the two other excited states have negligible contributions.

Sequential calculations have been performed to check the possible contribution of the deuteron transfer via the ^{63}Cu(^{18}O, ^{19}F)^{62}Ni reaction. Once again, microscopic spectroscopic information obtained with code NUSHELLX has been used. This procedure seems to be adequate since the calculations using this code have already proven to reproduce the spectroscopic information of neighboring isotopes for the one-proton-transfer reaction. Such calculations resulted in cross section values about five orders of magnitude below experimental data, which indicates that these data come mainly from the single-proton transfer. So, as the deuteron transfers have very low cross sections, they are not shown in Fig. 8.

When the proton pick-up is included in the complete CRC calculation discussed before, it does not affect significantly the theoretical QEBD, nor the EF. A comparison of this calculation with the other that considers only the inelastic channels plus the reorientation effect results in a small decrease of the χ^2_{red} value from 3.3 to 3.2. As the proton pick-up almost does not affect the QEBD and the EF, it is not shown in Fig. 7 to permit a better visualization of the other results.

E. α transfer

The experimental spectrum shown in Fig. 1 presents a group of events with $Z = 6$, which was assumed to be produced by the α-stripping process. The experimental excitation function of this process is shown in Fig. 9. For the α-stripping process, it is not possible to use the NUSHELLX code to obtain the spectroscopic information necessary to perform CRC calculations. In fact, structural α-transfer calculations are very difficult to be done and demand very specific experiments to observe their usually low cross sections. However, the observation and description of such channel were not the main purposes of this paper. So, an approximate theoretical treatment was adopted by using the extreme cluster model that considers the α particle as a valence particle, with zero spin, associated to the ^{14}C core. All the discussions about the CRC calculations made before are still valid in the present case. All channels of the ^{67}Gd with excitation energy below 3.2 MeV have been included in the calculations, for which the value SA = 0.2 has been settled by all channels. The result is shown in Fig. 9, where one can see that the data are well reproduced by the calculations, despite all approximations assumed. However, when the α-ß stripping channel is included in the complete CRC calculation discussed before, its contribution is negligible, and it was not shown in Fig. 7.

The results obtained in this paper are in qualitative accordance with those reported in the literature for neighboring systems, such as ^{16}O + ^{58,62}Ni [34], ^{16}O + ^{63}Cu [8], ^{16}O + ^{58}Ni [6], ^{16}O + ^{64}Zn [7], and ^{17}O + ^{64}Zn [9]. The first one, by Keeley *et al.*, measured a fusion barrier distribution (FBD) that was compared with theoretical calculations, while the other papers measured QEBD's to study the influence of

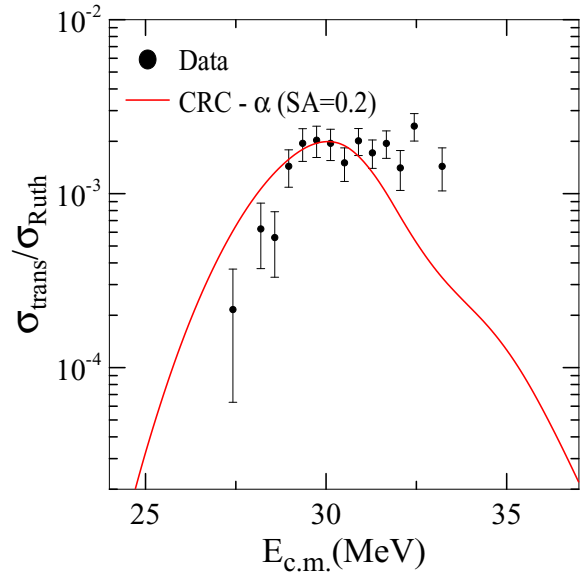

FIG. 9. α-transfer data. The red line represents the sums of the first 21 states of the ^{67}Gd nucleus.

the different reaction channels in the reaction mechanism. However, a direct comparison between the measured FBD and the QEBD for the $^{16}O + ^{58}Ni$ system has already been done in Ref. [6] and a remarkable similarity was found between their shapes. All papers cited above performed calculations with the same theoretical approach described in Sec. III, and they have shown that the inelastic channels are more relevant than the transfer channels in the reaction dynamics of the systems cited above. Besides, it was observed that the inclusion of the lower excited states changed mainly the heights of the barrier distributions, while the most excited ones [such as the ^{16}O (3^-) state] change their centroid positions. To complete this systematic study, we are going to measure the QEBD's for the $^{16,18}O + ^{65}Cu$ and $^{18}O + ^{64}Zn$.

IV. CONCLUSIONS

The precise quasielastic excitation function of the $^{18}O + ^{63}Cu$ reaction has been measured at energies around the Coulomb barrier, and its correspondent quasielastic barrier distribution has been derived. The experiment has been successfully performed at the Pelletron Accelerator of the University of São Paulo. The detector system employed permitted us to identify in the experimental spectra events coming from elastic scattering, inelastic excitations of target and projectile, and some transfer channels (mainly two neutrons, proton, and α), for which were measured their respective excitation functions. Extensive coupled channel and coupled reaction channel calculations have been performed, as well as shell-model structure calculations to obtain microscopic spectroscopic amplitudes for the overlaps involved in the reactions. The quasielastic barrier distribution has proved to be a helpful tool to analyze the competition between different reaction channels.

The coupled channel calculations showed that the first three excited states of the target ($1/2^-$, $5/2^-$, and $7/2^-$) and the 2^+ ($E = 1.982$ MeV) excitation of projectile were the most important ones to be inserted in the coupled channel calculations. Besides them, the reorientation of the ground state of the target also has a significant effect on the reaction mechanism. On the other hand, the inclusion of the transfer channels in the coupled reaction channel calculations showed that the one-neutron stripping, the α stripping, and the proton-pick-up do not play a significant role in the reaction mechanism. In the case of the neutron and proton transfers, microscopic spectroscopic amplitudes have been obtained and showed themselves consistent with the values reported in the literature. The CRC calculations for proton and α transfer gave a good description of the respective experimental transfer excitation functions. Finally, it was shown that the two-neutron transfer is the most important transfer channel in this system, as was shown by its large influence on the QEBD. An average spectroscopic amplitude of 0.7 has been adopted for describing the two-neutron transfer, and the CRC calculation has given a very good description of the experimental two-neutron-transfer excitation function. The extensive calculation of this paper suggests that the pairing effect of the peripheral two neutrons of the ^{18}O plays an important role in the transfer process of the $^{18}O + ^{63}Cu$ system.

ACKNOWLEDGMENTS

This work was financially supported by Fapesp, CNPq (Proc. No. 464898/2014-5), Capes and Faperj. One of the authors, E.C., thanks the financial support from CNPq (Proc. No. 305228/2015-3). We would like to thank the technical staff of Pelletron Laboratory for assisting in the maintenance and operation of the accelerator.

APPENDIX: NUSHELLX CALCULATIONS

NUSHELLX code has been used to describe the one-neutron stripping process. In the following calculations, it is important to remember that a shell model is being used, although, limitations on the description of some levels may occur (i.e., very collective states are expected not to be well described). In all structure calculations, it is also important to have both overlapping nuclei described in the same model space and with the same nuclear interaction (as they differ by only one neutron or two neutrons). A cross check of the results of shell-model calculation must be performed to verify if the theoretical order of appearance of the states and its energy coincide, within some uncertainty, with the experimental values. Shell-model codes have an accuracy of about 200 keV in the determination of the energy of the levels. So, states that are energetically close to each other may have their order of appearance interchanged.

The spectroscopic amplitudes for the $\langle ^{17}O|^{18}O\rangle$ overlaps were taken from Ref. [35]. The calculations used the *p-sd* model space, spanned by the $1p_{1/2}$, $1p_{3/2}$, $1d_{3/2}$, $1d_{5/2}$, and $2s_{1/2}$ orbitals, and neutrons and protons are considered separately. The interaction used in the calculations is the one proposed in Ref. [36], which is a modified version of the *psdwbt* interaction. Such interaction was found proper to describe oxygen isotopes and nuclei close to the $N = Z = 8$ magic numbers. In this mass region, the description of the coexistence of spherical and deformed shapes [37] has always represented a challenge for theoretical calculations. The obtained final interaction changes the intershell gap to properly describe the multiparticle-multihole states around this mass region for several of the oxygen isotopes. In NUSHELLX code, this interaction is labeled as *psdmod*. We used spectroscopic amplitudes reported in Table IV of Ref. [35]. They are very similar to the ones calculated with ZBM interaction [38] reported in Ref. [21].

The states of the $^{63,64}Cu$ nuclei were calculated with the fp model space, which is spanned by the $1f_{7/2}$, $2p_{3/2}$, $1f_{5/2}$, and $2p_{1/2}$ orbitals. Once again, the neutrons and protons have been considered separately. The interaction used in these calculations was the one reported in Ref. [39], originally developed to describe nuclei with masses around 41–49. After that, it has been demonstrated [40] that such interaction could be used for heavier nuclei (up to $A = 66$), including copper isotopes. In NUSHELLX code, this interaction is called *fpd6npn*. Because of computational limitations, the number of free nucleons to be distributed in the used model space had to be limited, by using the ^{58}Ni isotope as a core. Tests were performed using lighter nuclei (such as $^{54,56}Fe$), which result in no relevant differences. The derived SA are shown in Table II.

Due to the similarity and vicinity of the oxygen/fluorine and cooper/nickel isotopes, the structural calculations can be performed using the same model spaces and interactions adopted for the one-neutron-transfer process explained above. The SA used in CRC calculations are shown in Table III.

[1] M. V. Andres, N. Rowley, and M. A. Nagarajan, Phys. Lett. B **202**, 292 (1988).
[2] N. Rowley, G. R. Satchler, and P. H. Stelson, Phys. Lett. B **254**, 25 (1991).
[3] A. T. Kruppa, P. Romain, M. A. Nagarajan, and N. Rowley, Nucl. Phys. A **560**, 845 (1993).
[4] H. Timmers, J. R. Leigh, M. Dasgupta, D. J. Hinde, R. C. Lemmon, J. C. Mein, C. R. Morton, J. O. Newton, and N. Rowley, Nucl. Phys. A **584**, 190 (1995).
[5] H. Timmers, D. Ackermann, S. Beghini, L. Corradi, J. H. He, G. Montagnoli, F. Scarlassara, A. M. Stefanini, and N. Rowley, Nucl. Phys. A **633**, 421 (1998).
[6] R. F. Simões, D. S. Monteiro, L. K. Ono, A. M. Jacob, J. M. B. Shorto, N. Added, and E. Crema, Phys. Lett. B **527**, 187 (2002).
[7] J. F. P. Huiza, E. Crema, D. S. Monteiro, J. M. B. Shorto, R. F. Simões, N. Added, and P. R. S. Gomes, Phys. Rev. C **75**, 064601 (2007).
[8] J. M. B. Shorto, E. Crema, R. F. Simões, D. S. Monteiro, J. F. P. Huiza, N. Added, and P. R. S. Gomes, Phys. Rev. C **78**, 064610 (2008).
[9] J. F. P. Huiza, E. Crema, A. Barioni, D. S. Monteiro, J. M. B. Shorto, R. F. Simões, and P. R. S. Gomes, Phys. Rev. C **82**, 054603 (2010).
[10] E. Crema, D. R. Otomar, R. F. Simões, A. Barioni, D. S. Monteiro, L. K. Ono, J. M. B. Shorto, J. Lubian, and P. R. S. Gomes, Phys. Rev. C **84**, 024601 (2011).
[11] E. Crema, M. A. G. Alvarez, N. H. Medina, L. R. Gasques, J. F. P. Huiza, B. Fernández, Z. Abou-Haïdar, P. N. de Faria, P. R. S. Gomes, J. Lubian, and D. Verney, Phys. Rev. C **88**, 044616 (2013).
[12] M. Dasgupta, D. J. Hinde, N. Rowley, and A. M. Stefanini, Annu. Rev. Nucl. Sci. **48**, 401 (1998).
[13] M. Evers, M. Dasgupta, D. J. Hinde, D. H. Luong, R. Rafiei, R. du Rietz, and C. Simenel, Phys. Rev. C **84**, 054614 (2011).
[14] L. Corradi, G. Pollarolo, S. Szilner *et al.*, J. Phys. G: Nucl. Part. Phys. **36**, 113101 (2009).
[15] D. C. Rafferty, M. Dasgupta, D. J. Hinde, C. Simenel, E. C. Simpson *et al.*, Phys. Rev. C **94**, 024607 (2016).
[16] G. Potel, F. Barranco, E. Vigezzi, and R. A. Broglia, Phys. Rev. Lett. **105**, 172502 (2010).
[17] G. Potel, F. Barranco, F. Marini, A. Idini, E. Vigezzi, and R. A. Broglia, Phys. Rev. Lett. **107**, 092501 (2011).
[18] J. A. Lay, L. Fortunato, and A. Vitturi, Phys. Rev. C **89**, 034618 (2014).
[19] B. Paes, G. Santagati, R. Magana Vsevolodovna *et al.*, Phys. Rev. C **96**, 044612 (2017).
[20] D. Carbone, J. L. Ferreira, F. Cappuzzello, J. Lubian, C. Agodi *et al.*, Phys. Rev. C **95**, 034603 (2017).
[21] M. J. Ermamatov, R. Linares, J. Lubian, J. L. Ferreira, F. Cappuzzello *et al.*, Phys. Rev. C **96**, 044603 (2017).
[22] L. C. Chamon, B. V. Carlson, L. R. Gasques, D. Pereira, C. DeConti, M. A. G. Alvarez, M. S. Hussein, M. A. Candido Ribeiro, E. S. Rossi, and C. P. Silva, Phys. Rev. C **66**, 014610 (2002) and references therein.
[23] I. J. Thompson, Comput. Phys. Rep. **7**, 167 (1988).
[24] B. A. Brown and W. D. M. Rae, Nucl. Data Sheets **120**, 115 (2014).
[25] M. A. G. Alvarez, L. C. Chamon, L. C. Chamon, G. P. A. Nobre, T. Correa, M. S. Hussein, D. Pereira, Nucl. Phys. A **723**, 93 (2003).
[26] L. R. Gasques, L.C. Chamon, P. R. S. Gomes, and J. Lubian, Nucl. Phys. A **764**, 135 (2006).
[27] D. Pereira, C. P. Silva, J. Lubian, E. S. Rossi, Jr., L. C. Chamon, G. P. A. Nobre, and T. Correa, Nucl. Phys. A **826**, 211 (2009).
[28] http://www.nndc.bnl.gov/ensdf/, accessed on 11/20/2017.
[29] N. J. Stone, At. Data Nucl. Data Tables **90**, 75 (2005).
[30] S. Raman, C. W. Nestor, and P. Tikkanen, At. Data Nucl. Data Tables **78**, 1 (2001).
[31] D. M. Brink, Phys. Lett. B **40**, 37 (1972).
[32] A. Terakawa, H. Orihara, M. Oura, M. Hosaka *et al.*, Phys. Rev. C **66**, 064313 (2002).
[33] W. N. Wang and E. J. Winhold, Phys. Rev. **140**, B882 (1965).
[34] N. Keeley, J. S. Lilley, J. X. Wei, M. Dasgupta, D. J. Hinde *et al.*, Nucl. Phys. A **628**, 1 (1998).
[35] M. J. Ermamatov, F. Cappuzzello, J. Lubian, M. Cubero, C. Agodi *et al.*, Phys. Rev. C **94**, 024610 (2016).
[36] Y. Utsuno and S. Chiba, Phys. Rev. C **83**, 021301(R) (2011).
[37] J. L. Wood, K. Heyde, W. Nazarewicz, M. Huyse, and P. Van Duppen, Phys. Rep. **215**, 101 (1992).
[38] A. P. Zuker, B. Buck, and J. B. McGrory, Phys. Rev. Lett. **21**, 39 (1968).
[39] W. A. Richter, M. G. van der Merwe, R. E. Julies, and B. A. Brown, Nucl. Phys. A **523**, 325 (1991).
[40] M. G. van der Merwe, W. A. Richter, and B. A. Brown, Nucl. Phys. A **579**, 173 (1994).